INTERNATIONAL JOURNAL FOR NUMERICAL METHODS IN FLUIDS, VOL. 18, 721–731 (1994)

GENERALIZED INTEGRAL TRANSFORM SOLUTION FOR BOUNDARY LAYER FLOW OVER A SPHERE

P. L. C. LAGE* AND R. H. RANGEL

Department of Mechanical and Aerospace Engineering, University of California, Irvine, CA 92717, USA

SUMMARY

The generalized integral transform technique is applied to the boundary layer equations for flow over a sphere in their primitive variables. Even though a diffusion-based eigenvalue problem is used, the velocity profile, shear stress and separation point have been calculated with high accuracy. Low-order approximations are shown to be accurate near the surface and the predictions of the separation point is very good. Comparison with finite difference results shows the better convergence behaviour of the integral transform method.

KEY WORDS Generalized integral transform technique Boundary layer Sphere

1. INTRODUCTION

The application of integral transformations in the solution of linear diffusive problems is well known and has been reviewed by Mikhailov and Özişik.[1] Recently a generalization of the integral transform method has been developed and successfully applied to diffusion–convection problems.[2,3] The application of this method to partial differential equations has some similarity to the method of lines and spectral methods, because it transforms all the existing derivatives (except those in the parabolic direction) into algebraic terms. This procedure generates a system of ordinary differential equations which can be readily integrated. However, the generalized integral transform approach analytically operates the equations using an integral transformation. This transformation is generated by an eigenvalue problem based on the original set of equations, including the diffusive terms and, sometimes, convective terms. It represents the unknown functions using exact infinite series expansions in terms of the orthogonal set of eigenfunctions. Thus the unknown function dependence on all but one of the independent variables is known analytically. This enables one to use the series truncation error to monitor the accuracy of the solution during the integration procedure. Since ordinary differential equation solvers are extremely reliable and powerful nowadays, this method avoids completely the problems of stability and internal iterative procedures present in the finite difference solutions of non-linear partial differential equations. Although the generalized integral transform technique still has some shortcomings, e.g. some inability in handling non-homogeneous boundary conditions, it is undoubtedly a powerful method of solving partial differential equations.

The generalized integral transform method has been applied to convective heat transfer in ducts,[4–6] parabolic diffusion problems in finite domains[7,8] and the Navier–Stokes equations in a square cavity.[9] Its application to parabolic diffusion problems in external domains is the aim

* On leave from the Department of Chemical Engineering, COPPE/UFRJ, Brazil.

CCC 0271–2091/94/080721–11

Received April 1993
Revised November 1993

of the present work. The constant-property boundary layer equations constitute a well-known problem which is parabolic diffusive in terms of its primitive variable (the velocity components). Moreover, it is a convection-dominated problem with a non-homogeneous boundary condition at infinity, which represents a challenge to the application of the integral transform method. Thus it has been chosen as the working problem to illustrate the application of the finite integral transform method to parabolic diffusive partial differential equations in infinite domains.

2. ANALYSIS

The constant-density boundary layer equations for flow over axisymmetric bodies are given by Schlichting.[10] When curvature effects are neglected, they can be written in the dimensionless form

$$\frac{1}{\zeta}\frac{\partial}{\partial \xi}(\zeta U) + \frac{\partial V}{\partial \eta} = 0, \tag{1}$$

$$U\frac{\partial U}{\partial \xi} + V\frac{\partial U}{\partial \eta} = g(\xi) + \frac{\partial^2 U}{\partial \eta^2}, \tag{2}$$

where

$$\zeta(\xi) = \sin \xi, \tag{3}$$

$$g(\xi) = \tfrac{9}{8}\sin(2\xi), \tag{4}$$

with the boundary conditions

$$\begin{gathered} \eta = 0: \quad U = 0, \quad V = 0, \\ \eta \to \infty: \quad U = U_e(\xi) \to \tfrac{3}{2}\sin \xi \quad \text{or} \quad \partial U/\partial \eta \to 0, \\ \xi = 0: \quad U = 0, \end{gathered} \tag{5}$$

where all the symbols are as defined in Appendix II.

In order to generate an integral transformation through the infinite series of orthogonal solutions of a homogeneous eigenvalue problem, the boundary conditions at infinity must be substituted by

$$\eta = H: \quad \partial U/\partial \eta = 0, \tag{6}$$

where H is a sufficiently large parameter. Thus, considering the diffusion term in equation (2), the following eigenvalue problem is built:

$$\begin{gathered} \mathrm{d}^2\psi_k/\mathrm{d}\eta^2 + \beta_k^2\psi_k = 0, \\ \eta = 0: \quad \psi_k = 0; \qquad \eta = H: \quad \partial\psi_k/\partial\eta = 0. \end{gathered} \tag{7}$$

This enables the development of the integral transform pair

$$U(\xi, \eta) = \sum_{k=1}^{\infty} \frac{1}{N_k^{1/2}}\psi_k(\eta)\overline{U_k}(\xi), \tag{8}$$

$$\overline{U_k}(\xi) = \frac{1}{N_k^{1/2}}\int_0^H \psi_k(\eta)U(\xi, \eta)\,\mathrm{d}\eta, \tag{9}$$

where

$$\psi_k(\eta) = \sin(\beta_k \eta), \qquad \beta_k = (2k - 1)\,\pi/2H, \quad k = 1, 2, \ldots, \tag{10}$$

whose norm is $N_k = 0.5H$ for every k.

Using equation (8), the continuity equation (1) can be transformed into

$$V(\xi, \eta) = -\frac{1}{\zeta} \sum_{k=1}^{\infty} f_k(\eta) \frac{\partial}{\partial \xi} (\zeta \overline{U_k}), \tag{11}$$

where f is as defined in Appendix I.

The integral transformation of the momentum equation (2), using equation (8) to express the non-linear terms and equation (11), produces the following infinite set of non-linear ordinary differential equations:

$$\sum_{j=1}^{\infty} \sum_{i=1}^{\infty} (A_{kji} - F_{kij}) \overline{U_j} \frac{d\overline{U_i}}{d\xi} = \cot \xi \sum_{j=1}^{\infty} \sum_{i=1}^{\infty} F_{kji} \overline{U_i U_j} + g(\xi) P_k - \beta^2 \overline{U_k}, \quad k = 1, 2, \ldots, \tag{12}$$

where A, F and P are as defined in Appendix I. In order to be numerically solvable, this system must be truncated at some value, say $k = N$. The resulting finite system of non-linear differential equations is amenable for numerical integration along the ξ-variable. However, it should be noticed that equation (12) vanishes identically for $\overline{U_k} = 0$ for every k, i.e. when $U = 0$. Accordingly, the integration cannot be started at $\xi = 0$. In order to overcome this limitation, the stagnation point flow solution is evoked, which can be expressed in the form

$$U = \tfrac{3}{2}\xi \, d\phi/d\eta, \tag{13}$$

$$\tfrac{2}{3}\phi''' + 2\phi\phi'' + 1 - \phi'^2 = 0, \tag{14}$$

$$\eta = 0: \quad \phi = 0, \quad \phi' = 0; \qquad \eta \to \infty: \quad \phi' = 1,$$

where the primes denote differentiation with respect to η. The boundary condition at infinity is also imposed at $\eta = H$ in order to solve equation (14) numerically.

3. NUMERICAL PROCEDURE

Firstly, equation (14) is solved by a finite difference scheme with a non-uniform adaptive grid which is able to return grid point values for any desired accuracy. Then trapezoidal quadrature based on these grid points and equation (13) are used to calculate the transformed velocity components $\overline{U_k}$, from the integral transform definition (9) at a point close to $\xi = 0$. It has been verified that the results do not vary as long as the starting ξ-value remains small ($\xi = 0.01$ was usually adopted for the starting point). Moreover, care has been taken to use enough points per period of the eigenfunctions in order to guarantee good precision in the quadrature integration for determining the $\overline{U_k}$ initial values. A relative precision 10^{-6} was typically required, which generated a grid with 2000–3000 points.

The system of ordinary differential equations given by (12), truncated to N terms in the summations, was treated as a differential algebraic system of equations and its numerical integration was carried out using DAWRS (differential algebraic wave-form relaxation solver).[11,12] The system Jacobian was calculated analytically and the results obtained were identical to those obtained when DAWRS was allowed to approximate the Jacobian by finite differences. The required relative precision during the integrations was typically 10^{-6}. The integration was performed up to the separation point. At this point, for large N-values, the DAWRS corrector

step was unable to converge. This seems to be caused by the breakdown of the assumptions which lead to the boundary layer equations, which are no longer valid. However, it was possible to integrate as close as desired to the separation point. The values obtained for the normal derivative of the dimensionless tangential velocity component at the surface and at a point close to the separation point were typically of the order of 10^{-2}–10^{-3}. Since this derivative decreases very sharply near the separation point, there is no appreciable difference between the last integration point and the separation point.

The integral transform solution was compared with a finite difference solution of the same set of equations (equation (1), (2) and (5) but with a different boundary condition for the external flow ($U = U_e$ at $\eta = H$). A fully implicit scheme with a uniform grid in η was marched in the ξ-direction using uniform 0.05 increments. A precision of four figures was required in the inner loop for evaluation of the non-linear terms.

The value chosen for H has been varied until convergence was achieved. It should be pointed out that although a large H-value brings the assumed boundary condition closer to the true one, it is desirable to have the smallest possible H-value. The reason is the increase in computational effort due to an increase in the number of grid points in the finite difference solution and in the number of eigenfunctions in the integral transform solution. A value $H = 6$ was shown to be appropriate.

4. RESULTS AND DISCUSSION

Figures 1–3 show the convergence behaviour of the dimensionless velocity profile $U(\eta)$ at $\xi = \pi/6$, $\pi/3$ and $\pi/2$ respectively with increasing N. It is clear that the even-N series expansions converge

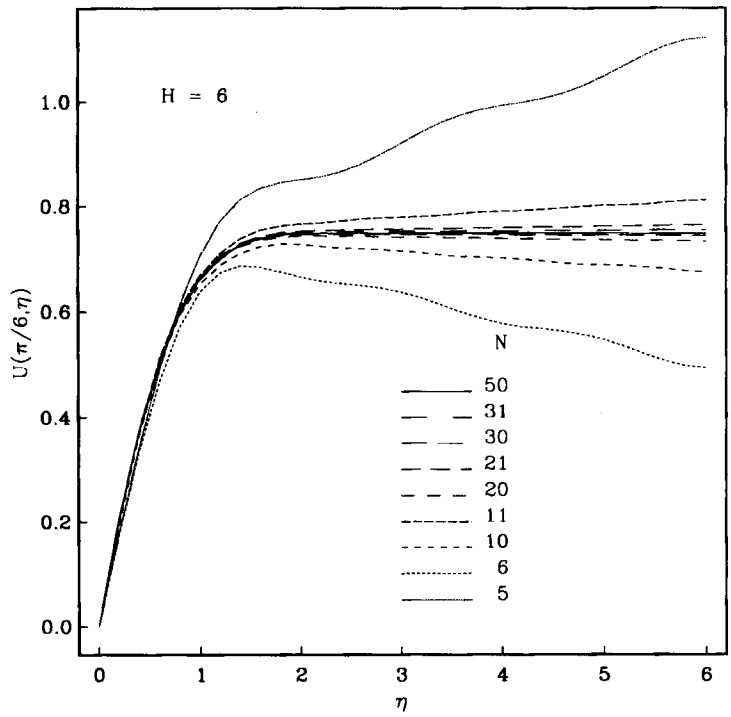

Figure 1. Dimensionless tangential velocity profile at $\xi = \pi/6$

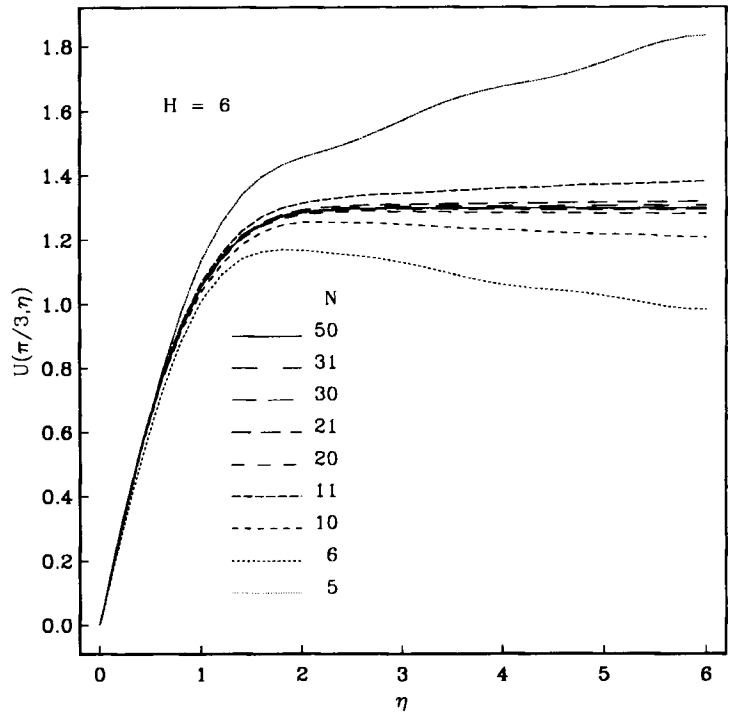

Figure 2. Dimensionless tangential velocity profile at $\xi = \pi/3$

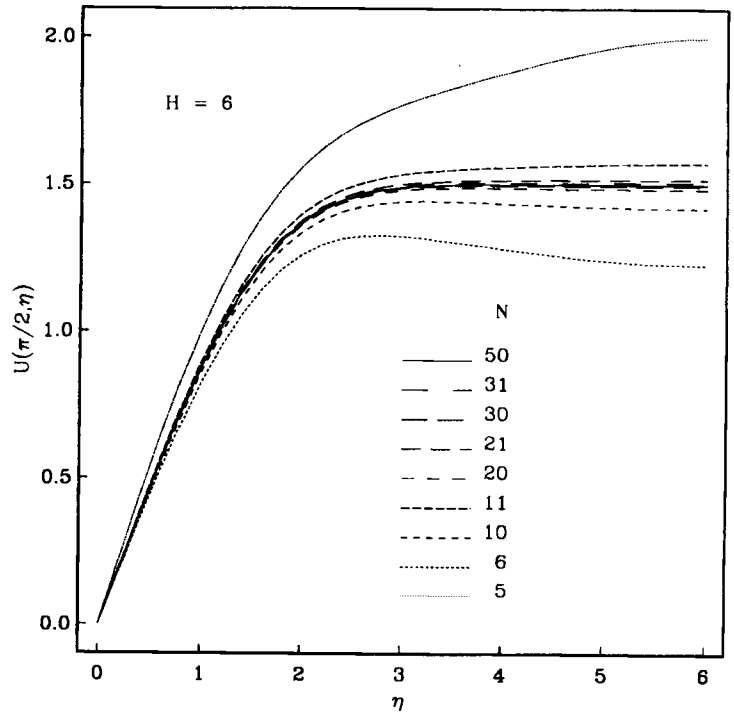

Figure 3. Dimensionless tangential velocity profile at $\xi = \pi/2$

to the exact solution from below whereas the odd-N series expansions converge to it from above. Besides, the even-N series expansions have a slightly better convergence behaviour than the odd-N series expansions. The oscillatory character of the solution for small N is evidently caused by the series expansion in sine functions. Tables I–III give the $U(\eta)$-profiles for $\xi = \pi/6$, $\pi/3$ and $\pi/2$ respectively for the integral transform solution using 20, 40 and 50 eigenfunctions and for the finite difference (FD) solution using 31 and 61 grid points in the η-direction. The convergence of the U series expansion (equation (9)) is also shown by the maximum relative value of the last term in relation to the overall series value (which gives an idea of the truncation error in the series summation). It is interesting to notice that the ideal flow solution at $\eta = H$ is imposed on the finite-difference method but is not the boundary condition in the integral transform method. Thus the accuracy of the integral transform solution can be inferred by comparison of the U-value at the outer boundary and the ideal flow solution. Comparing the results for the two numerical methods, the better convergence behaviour of the integral transform method is clear through the accuracy of its lower-order approximations near the surface. Besides, the integral transform solution with 40 terms, when compared with the 50-term solution, is accurate to three figures almost everywhere.

Figure 4 shows the convergence behaviour of the dimensionless normal derivative of the tangential velocity at the surface with increasing N. This derivative is related to the shear stress at the surface by

$$\left(\frac{\partial U}{\partial \eta}\right)_{\eta=0} = Re^{1/2}\,\frac{\tau_s}{\rho u_\infty^2}. \tag{15}$$

Table I. Dimensionless tangential velocity profiles for $\xi = \pi/6$ ($H = 0{\cdot}6$)

η	U			U (FD)	
	N			No. of points	
	20	40	50	31	61
0·00	0·0000	0·0000	0·0000	0·0000	0·0000
0·20	0·2056	0·2067	0·2065	0·2105	0·2065
0·40	0·3742	0·3740	0·3741	0·3801	0·3733
0·60	0·5018	0·5036	0·5038	0·5094	0·5014
0·80	0·5969	0·5983	0·5984	0·6020	0·5943
1·00	0·6611	0·6627	0·6628	0·6636	0·6572
1·20	0·7006	0·7032	0·7034	0·7014	0·6966
1·40	0·7242	0·7268	0·7270	0·7227	0·7195
1·60	0·7362	0·7391	0·7394	0·7336	0·7317
1·80	0·7412	0·7450	0·7454	0·7389	0·7379
2·00	0·7436	0·7476	0·7480	0·7414	0·7409
3·00	0·7419	0·7487	0·7494	0·7451	0·7450
4·00	0·7392	0·7483	0·7491	0·7471	0·7471
5·00	0·7365	0·7479	0·7489	0·7487	0·7487
6·00	0·7336	0·7475	0·7487	0·7500	0·7500
Maximum relative contribution of $\overline{U_N}$					
—	0·0014	0.0001	3×10^{-5}	—	—

Table II. Dimensionless tangential velocity profiles for $\xi = \pi/3$ ($H = 0{\cdot}6$)

η	U			U (FD)	
	N			No. of points	
	20	40	50	31	61
0·00	0·0000	0·0000	0·0000	0·0000	0·0000
0·20	0·2906	0·2919	0·2917	0·2935	0·2899
0·40	0·5430	0·5433	0·5435	0·5463	0·5395
0·60	0·7511	0·7535	0·7539	0·7564	0·7474
0·80	0·9201	0·9224	0·9226	0·9234	0·9136
1·00	1·0485	1·0512	1·0515	0·1496	1·0402
1·20	1·1403	1·1442	1·1446	1·1397	1·1316
1·40	1·2035	1·2076	1·2080	1·2003	1·1940
1·60	1·2432	1·2480	1·2484	1·2385	1·2340
1·80	1·2661	1·2719	1·2724	1·2611	1·2581
2·00	1·2790	1·2852	1·2857	1·2738	1·2719
3·00	1·2872	1·2971	1·2980	1·2876	1·2874
4·00	1·2840	1·2968	1·2979	1·2907	1·2907
5·00	1·2813	1·2964	1·2977	1·2944	1·2944
6·00	1·2792	1·2961	1·2975	1·2990	1·2990
Maximum relative contribution of $\overline{U_N}$					
—	0·0010	6×10^{-5}	2×10^{-5}	—	—

Table III. Dimensionless tangential velocity profiles for $\xi = \pi/2$ ($H = 0{\cdot}6$)

η	U			U (FD)	
	N			No. of points	
	20	40	50	31	61
0·00	0·0000	0·0000	0·0000	0·0000	0·0000
0·20	0·1853	0·1859	0·1860	1·1808	0·1857
0·40	0·3689	0·3702	0·3704	0·3613	0·3702
0·60	0·5474	0·5495	0·5497	0·5385	0·5499
0·80	0·7165	0·7193	0·7195	0·7074	0·7199
1·00	0·8719	0·8753	0·8756	0·8627	0·8749
1·20	1·0099	1·0139	1·0143	1·0002	1·0111
1·40	1·1282	1·1329	1·1333	1·1172	1·1263
1·60	1·2260	1·2312	1·2317	1·2128	1·2199
1·80	1·3037	1·3094	1·3100	1·2881	1·2934
2·00	1·3629	1·3693	1·3698	1·3452	1·3491
3·00	1·4778	1·4871	1·4879	1·4606	1·4617
4·00	1·4853	1·4975	1·4985	1·4767	1·4775
5·00	1·4834	1·4975	1·4987	1·4828	1·4832
6·00	1·4826	1·4974	1·4987	1·5000	1·5000
Maximum relative contribution of $\overline{U_N}$					
—	7×10^{-6}	4×10^{-7}	1×10^{-7}	—	—

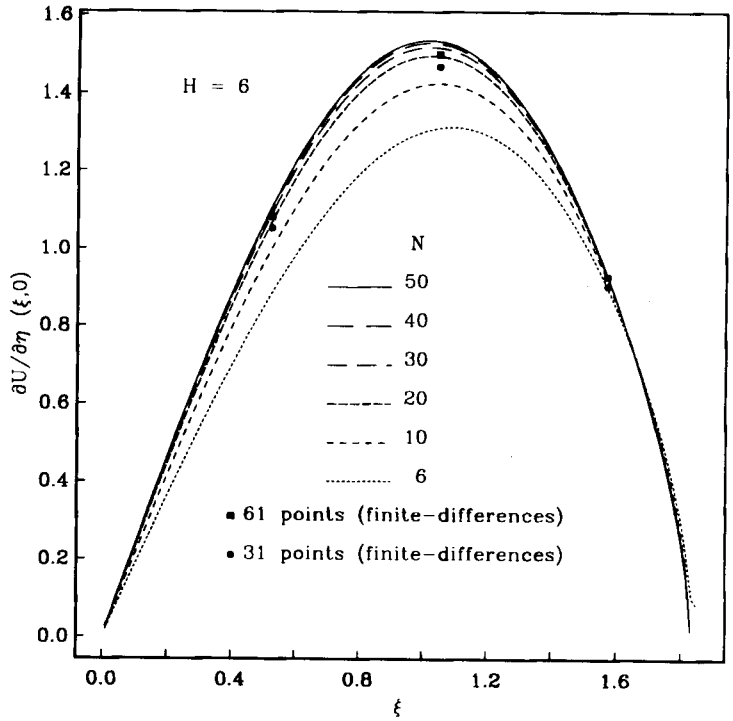

Figure 4. Dimensionless shear stress at surface

The dimensionless derivative values prediced by the finite difference solution using 31 and 61 grid points are also shown in Figure 4 for $\xi = \pi/6$, $\pi/3$ and $\pi/2$. It can be seen that the integral transform solution for $N = 20$ is as accurate as the finite difference solution with 61 grid points. Since this derivative is calculated analytically in the integral transform method whereas it is fully numerical in the finite difference solution, its prediction by the integral transform method was expected to be much more accurate.

Table IV gives the values for the separation point obtained using the integral transform solution with several values of N. It should be noted that for $N = 6$ the separation point was considered to be the point where the tangential velocity derivative at the surface reached a minimum. At this small N-value the solution obtained is not good enough to predict the

Table IV. Separation point values predicted by integral transform solution

N	Separation point (deg)
6	105·5
10	104·7
20	104·9
30	105·0
40	104·8
50	104·8

derivative values well. However, the separation point determined through this consideration is in good agreement with the values obtained for larger N. Moreover, the converged value of 104.8° agrees remarkably well with the most accurate value obtained by finite differences cited by White,[13] which is 105.5°.

5. CONCLUSIONS

The generalized integral transform technique has been applied to the boundary layer equations in primitive variables and the results compared with those obtained by the finite difference solution for the same set of equations but with the boundary condition for external flow. Similarly to other numerical methods, the condition at infinity was applied to a finite but sufficiently far distance from the surface. In this way the integral transform method based on finite domains could be applied to a problem with an infinite domain. Although applied to a parabolic system where convection is extremely important, the generalized integral transform technique based on a diffusive eigenvalue problem has proved to be accurate and reliable. Its low-order approximations are able to predict accurately the velocity profile near the surface and the separation point. High-order approximations predict the velocity profile and shear stress at the surface with high accuracy. Moreover, it has shown better convergence characteristics than the finite difference method. However, further improvement in the eigenvalue problem by the inclusion of a convective term is possible and might lead to even better convergence behaviour.

ACKNOWLEDGEMENTS

One of the authors (P.L.C. L.) would like to acknowledge the financial support from CNPq, Grant 202129/90.0. Helpful discussions with Professor R. M. Cotta from COPPE/UFRJ are also acknowledged. DAWRS, version 1.0, was kindly provided by A. R. Secchi. The finite difference calculations were performed by F. Pannebaker.

APPENDIX I

Several auxiliary variables have been used in the analysis section to simplify the notation. They are defined below and their analytically calculated values are also given:

$$f_k = \frac{1}{N_k^{1/2}} \int_0^{\eta} \psi_k(\eta')\, \mathrm{d}\eta' = \sqrt{\left(\frac{2}{H}\right)} \frac{1}{\beta_k} (1 - \cos \beta_k \eta), \tag{16}$$

$$P_k = \frac{1}{N_k^{1/2}} \int_0^{H} \psi_k(\eta)\, \mathrm{d}\eta = \sqrt{\left(\frac{2}{H}\right)} \frac{1}{\beta_k}, \tag{17}$$

$$A_{ijk} = \sqrt{\left(\frac{1}{N_i N_j N_k}\right)} \int_0^{H} \psi_i(\eta)\psi_j(\eta)\psi_k(\eta)\, \mathrm{d}\eta$$

$$= \left(\frac{2}{H}\right)^{3/2} \frac{-2\beta_i\beta_j\beta_k + \beta_i(\beta_i^2 - \beta_j^2 - \beta_k^2)\cos[(\beta_i + \beta_j + \beta_k)H]}{\beta_i^4 + \beta_j^4 + \beta_k^4 - 2(\beta_i^2\beta_j^2 + \beta_i^2\beta_k^2 + \beta_j^2\beta_k^2)}, \tag{18}$$

$$F_{ijk} = \sqrt{\left(\frac{1}{N_i N_k}\right)} \int_0^{H} \psi_i(\eta) f_j(\eta) \frac{\mathrm{d}\psi_k}{\mathrm{d}\eta}\, \mathrm{d}\eta = \sqrt{\left(\frac{2}{H}\right)} \frac{1}{\beta_j} C_{ik} - \frac{1}{\beta_j^2} E_{ijk}, \tag{19}$$

where

$$C_{ik} = \sqrt{\left(\frac{1}{N_i N_k}\right)} \int_0^H \psi_i(\eta) \frac{\mathrm{d}\psi_k}{\mathrm{d}\eta} \mathrm{d}\eta$$

$$= \begin{cases} \dfrac{2}{H} \dfrac{\beta_k}{\beta_i^2 - \beta_k^2} \{\beta_i + \beta_k \cos[(\beta_i + \beta_k)H]\}, & i \neq k, \\ 1/H, & i = k, \end{cases} \tag{20}$$

$$E_{ijk} = \sqrt{\left(\frac{1}{N_i N_j N_k}\right)} \int_0^H \psi_i(\eta) \frac{\mathrm{d}\psi_j}{\mathrm{d}\eta}(\eta) \frac{\mathrm{d}\psi_k}{\mathrm{d}\eta}(\eta) \mathrm{d}\eta$$

$$= \left(\frac{2}{H}\right)^{2/3} \frac{\beta_i \beta_j \beta_k \{\beta_i^2 - \beta_j^2 - \beta_k^2 + 2\beta_j \beta_k \cos[(\beta_i + \beta_j + \beta_k)H]\}}{\beta_i^4 + \beta_j^4 + \beta_k^4 - 2(\beta_i^2 \beta_j^2 + \beta_i^2 \beta_k^2 + \beta_j^2 \beta_k^2)}. \tag{21}$$

APPENDIX II: NOMENCLATURE

A auxiliary variable
f auxiliary variable
F auxiliary variable
g dimensionless pressure term, $U_e \, \mathrm{d}U_e/\mathrm{d}\xi$
H dimensionless normal distance where the boundary condition at $\eta \to \infty$ is applied
N eigenfunction norm
P auxilary variable
r surface–axis-of-symmetry distance
Re Reynolds number, $u_\infty R/\nu$
u tangential velocity
u_e outer-flow tangential velocity (ideal flow)
u_∞ freestream velocity
U dimensionless tangential velocity, u/u_∞
U_e dimensionless outer-flow tangential velocity, u_e/u_∞
$\bar{U}$ integral-transformed dimensionless tangential velocity
v normal velocity
V dimensionless normal velocity, $\sqrt{(Re)}v/u_\infty$
x tangential co-ordinate
y normal co-ordinate

Greek letters

β eigenvalue
ζ dimensionless surface–axis-of-symmetry distance, r/R
η dimensionless normal co-ordinate, $\sqrt{(Re)}y/R$
ν kinematic viscosity
ξ dimensionless tangential co-ordinate, x/R
τ_s shear stress at surface
ϕ dimensionless streamfunction for stagnation point flow (equation (14))
ψ eigenfunction

REFERENCES

1. M. D. Mikhailov and M. N. Özişik, *Unified Analysis of Heat and Mass Diffusion*, Wiley, New York, 1984.
2. R. M. Cotta, *Integral Transforms in Computational Heat and Fluid Flow*, CRC Press, Boca Raton, FL, 1992.
3. M. D. Mikhailov and R. M. Cotta, 'Unified integral transform method,' *J. Braz. Soc. Mech. Sci.*, **12**, (4), 26–35 (1990).
4. R. O. C. Guedes and R. M. Cotta, 'Periodic laminar forced convection within ducts including wall heat conduction effects,' *Int. J. Eng. Sci.*, **29**, 535–547 (1991).
5. J. B. Aparecido and R. M. Cotta, 'Thermally developing laminar flow inside rectangular ducts,' *Int. J. Heat Mass Transfer*, **33**, 341–347 (1900).
6. J. B. Aparecido and R. M. Cotta, 'Laminar flow inside hexagonal ducts,' *Comput. Mech.* **6**, 93–100 (1990).
7. R. M. Cotta and T. M. B. Carvalho, 'Hybrid analysis of boundary layer equations for internal flow problems,' *Proc. 7th Conf. on Numerical Methods in Laminar and Turbulent Flow*, Stanford, CA, July 1991, pp. 106–115.
8. R. M. Cotta and R. Serfaty, 'Integral Transform Algorithm for Parabolic Diffusion Problems with Nonlinear Boundary and Equation Source Terms,' *Proc. 7th Int. Conf. on Numerical Methods in Laminar and Turbulent Flow*, Stanford, CA, July 1991, pp. 916–926.
9. J. S. Pérez Guerreiro and R. M. Cotta, 'Integral transform solution for the lid-driven cavity flow problem in stream function-only formulation,' *Int. j. numer. methods fluids*, **15**, 399–409 (1992).
10. H. Schlichting, *Boundary Layer Theory*, 7th edn. McGraw-Hill, New York, 1979, pp. 235–239.
11. A. R. Secchi, M. Morari and E. C. Biscaia Jr., 'DAWRS: a differential-algebraic system solver by the waveform relaxation method,' *Proc. Sixth Distributed Memory Computing Conf. (DMCC6)*, Portland, OR, April 1991.
12. A. R. Secchi, M. Morari and E. C. Biscaia Jr., 'The waveform relaxation method for concurrent dynamic process simulation,' *Proc. AIChE Meeting*, Los Angeles, CA, November 1991.
13. F. M. White, *Viscous Fluid Flow*, 2nd edn, McGraw-Hill, New York, 1991, pp. 293–298.